Macromolecules

PERSPECTIVE

pubs.acs.org/Macromolecules

Top-Down Multidimensional Mass Spectrometry Methods for Synthetic Polymer Analysis

Xiaopeng Li,[†] Li Guo,[‡] Madalis Casiano-Maldonado,[†] Donghui Zhang,[‡] and Chrys Wesdemiotis*[,†,‡]

[†]Department of Chemistry and [‡]Department of Polymer Science, The University of Akron, Akron, Ohio 44325, United States

[‡]Department of Chemistry and Macromolecular Studies Group, Louisiana State University, Baton Rouge, Louisiana 70803, United States

ABSTRACT: The ability of multidimensional mass spectrometry (MS) approaches, interfacing different ionization methods with tandem mass spectrometry (MS^2) fragmentation and ion mobility (IM) separation, to characterize synthetic polymers is demonstrated for poly(α-peptoid)s synthesized by N-heterocyclic carbene (NHC)-mediated zwitterionic ring-opening polymerization. Matrix-assisted laser desorption ionization (MALDI) causes elimination of the NHC initiator, if performed in the presence of cationizing salts. Electrospray ionization (ESI) is softer, allowing for the detection of the intact sample. It also shows that in proper solvents self-assembly of the poly(α-peptoid) occurs to form supramacromolecules; since these noncovalent self-assemblies overlap with the main product, separation by IM MS is essential for their conclusive identification. MS^2 confirms the connectivity of the poly(α-peptoid)s, whereas MS^2 combined with IM separation renders valuable insight into the binding interactions in the supramolecular assemblies and on the structures and conformations of the poly(α-peptoid) resulting after NHC elimination. Performing all analyses inside the mass spectrometer ("top-down") enables fast, sensitive, and cost-effective analysis of polymer composition, structure, and architecture without prior derivatization, separation, or degradation.

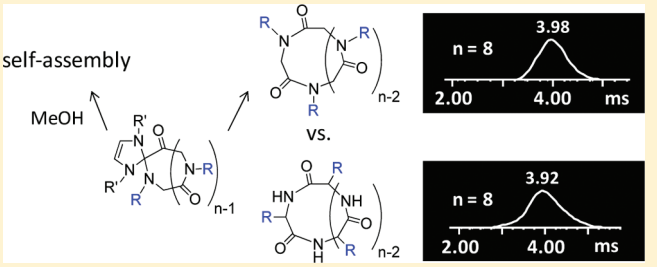

INTRODUCTION

The introduction of matrix-assisted laser desorption ionization (MALDI)[1,2] and electrospray ionization (ESI)[3] has enabled the formation of gas-phase ions from a wide variety of biomaterials and synthetic polymers, opening a new era for their mass spectrometry (MS) analysis. MS experiments provide the mass-to-charge ratios (m/z) of the constituent n-mers of a polymeric material, from which compositional heterogeneity, molecular weight, and functionality distributions can be deduced. Such information has been essential in the discovery of new polymerization techniques, the elucidation of polymerization mechanisms, and the advancement and commercialization of new products.[4−14] Nevertheless, significant challenges still exist. Both MALDI and ESI require the use of solvents and/or matrices that may alter the identity of reactive or labile analytes. Furthermore, polymerizations, in particular newly developed methods, may create complex mixtures that are difficult or impossible to characterize by single-stage MS because of discrimination effects in the ionization and detection steps and/or because the product contains isobaric components or a mixture of isomeric architectures that cannot be identified by m/z measurement alone, even at high mass resolution. In this Perspective, we will demonstrate how such problems can be bypassed by combining MALDI and ESI with two-dimensional (2-D) top-down methods involving tandem mass spectrometry (MS^2), i.e., two stages of mass analysis with intermediate fragmentation,[15−18] ion mobility mass spectrometry (IM MS), i.e., post-ionization gas-phase separation by mass, charge, and shape coupled with mass analysis,[19−31] or a 3-D combination thereof.[32,33] The "top-down" characteristic indicates structural identification entirely in the mass spectrometer without prior derivatization, degradation, or chromatographic separation; in contrast, "bottom-up" analysis includes one or more of the latter steps.

The system chosen to illustrate the challenges addressed by the mentioned multidimensional methods is cyclic poly(α-peptoid)s prepared via N-heterocyclic carbene (NHC)-mediated zwitterionic ring-opening polymerization.[34−37] As peptide mimics, poly(α-peptoid)s have shown promise as therapeutic agents or drug delivery carriers because of their enhanced hydrolytic stability compared to conventional polypeptides. For those examined in the present study, the major polymeric species observed was the NHC-containing poly(α-peptoid) by ESI, but either the NHC-bound poly(α-peptoid) or the free poly(α-peptoid) without the NHC functionality by MALDI, depending on the conditions used.[37] Several questions are raised by this discrepancy. Do the matrix and salt used in MALDI cause the loss of the NHC segment, or is ESI favoring the ionization of NHC-containing species? Did the ring-opening polymerization yield solely NHC-substituted poly(α-peptoid) or a mixture of this product plus unsubstituted material? Are the NHC-missing poly(α-peptoid) molecules cyclic or ring-opened isomers without end groups? Herein, we will examine this puzzling polymerization process at

Received: March 9, 2011
Revised: May 18, 2011
Published: June 07, 2011

Scheme 1. Synthesis of Poly(α-peptoid)s by N-Heterocyclic Carbene (NHC)-Mediated Zwitterionic Ring-Opening Polymerization

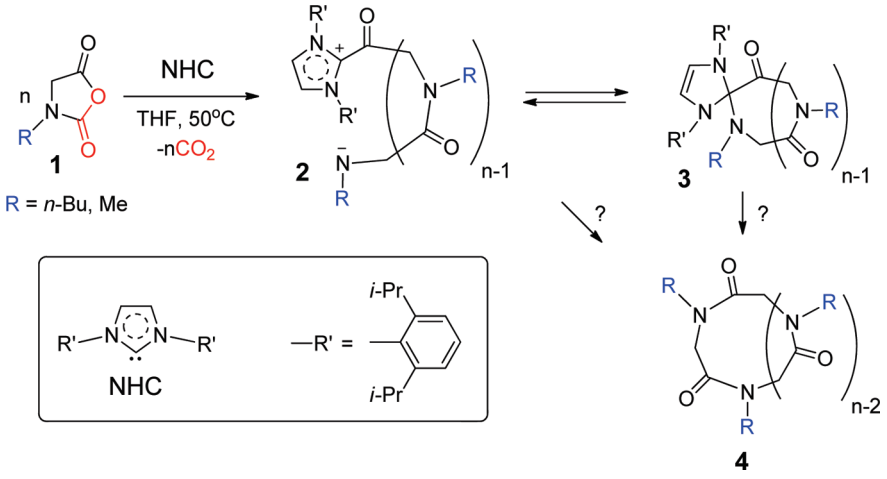

different levels of top-down mass spectrometry, using MALDI MS, MALDI MS^2, ESI MS, ESI MS^2, traveling wave ion mobility (TWIM) MS (a variant of IM MS),[27,29,30,38−41] and TWIM MS^2.

EXPERIMENTAL SECTION

Materials. The poly(α-peptoid)s, poly(*N*-butylglycine) (M_n 1500 or 1100 Da), and poly(*N*-methylglycine) (M_n 1800 Da) were synthesized via N-heterocyclic carbene (NHC)-mediated ring-opening polymerization (Scheme 1), as described by Guo and Zhang.[37] Cyclic poly(alanine), an isomer of poly(*N*-methylglycine), was prepared by the procedure of Zhou et al.[42] Chemicals and solvents were purchased from Fisher Scientific (Pittsburgh, PA) or Sigma/Aldrich (St. Louis, MO) and were used as received.

MALDI MS. The MALDI MS experiments were carried out on a Bruker Ultraflex III tandem time-of-flight (ToF/ToF) mass spectrometer (Bruker Daltonics, Billerica, MA), equipped with a Nd:YAG laser emitting at a wavelength of 355 nm. All spectra were measured in positive reflector mode. The instrument was calibrated externally with a poly(methyl methacrylate) standard prior to each measurement. Five different matrices were used: dithranol (DIT), 2,5-dihydroxybenzoic acid (DHB), and *trans*-2-[3-(4-*tert*-butylphenyl)-2-methyl-2-propenylidene]malononitrile (DCTB) dissolved in tetrahydrofuran (THF) at 20, 10, and 20 mg/mL, respectively, as well as 3-hydropicolinic acid (HPA) and α-cyano-4-hydroxycinnamic acid (CHCA) dissolved in acetonitrile (ACN)/water (v/v, 50/50) at 5 mg/mL. The polymer samples were dissolved in methanol (MeOH) at 5−10 mg/mL. Sodium trifluoroacetate (NaTFA), sodium iodide (NaI), and potassium trifluoroacetate (KTFA), which served as cationization salts, were dissolved in THF at 10 mg/mL each. Matrix and cationizing salt solutions were mixed in the ratio 10:1 (v/v). The samples were analyzed with and without the addition of cationization salt. Sample preparation involved depositing 0.5 μL of matrix/salt mixture or just matrix on the wells of a 384-well ground-steel plate, allowing the spots to dry, depositing 0.5 μL of each sample on top of a dry matrix (or matrix/salt) spot, and adding another 0.5 μL of matrix/salt or matrix on top of the dry sample (sandwich method); compared to the commonly used dry droplet method, in which a mixture of matrix and sample is deposited onto the target plate, the sandwich method minimizes the disintegration of labile substances and allows for facile variation of the matrix to maximize the signal intensity. MALDI MS^2 experiments were performed using Bruker's LIFT mode.[43] Data analysis was conducted with the flexAnalysis software.

ESI MS and ESI-TWIM MS. Both ESI MS and ESI-TWIM MS experiments were performed with a Waters Synapt HDMS quadrupole/time-of-flight (Q/ToF) mass spectrometer (Waters, Milford, MA).[38] The triwave region of this instrument, located between the Q and ToF mass analyzers, contains three confined regions in the order trap cell (closest to Q), TWIM cell, and transfer cell (closest to ToF). Either the trap or the transfer cell can be used for MS^2 studies via collisionally activated dissociation (CAD). The following ESI and TWIM parameters were selected: ESI capillary voltage, 3.5 kV; sample cone voltage, 35 V; extraction cone voltage, 3.2 V; desolvation gas flow, 500 L/h (N_2); trap collision energy (CE), 2 or 6 eV; transfer CE, 1 or 4 eV; trap gas flow, 1.5 mL/min (Ar); IM gas flow, 22.7 mL/min (N_2); sample flow rate, 5 μL/min; source temperature, 40 or 100 °C; desolvation temperature, 60 or 150 °C; traveling wave velocity, 350 m/s; traveling wave height, 8.5, 9.5, or 11 V, depending on the m/z ratio to be separated. The sprayed solutions were prepared by dissolving 0.3 mg of sample in 1 mL of MeOH or ethanol (EtOH)/ACN (v/v, 50/50). In select experiments, a few droplets of a 10 mg/mL NaTFA solution in the same solvent, or of trifluoroacetic acid, were added to the sprayed mixture. Conventional MS^2 (CAD) spectra were acquired in the trap cell with the TWIM device turned off. MS^2 (CAD) experiments combined with TWIM separation were performed in the trap cell (fragmentation before IM separation) or in the transfer cell (fragmentation after IM separation). All MS^2 studies employed 60 eV collisions with Ar targets. A more detailed description of our TWIM experiments can be found elsewhere.[29,30,33] Data analysis was conducted with the MassLynx 4.1 and DriftScope 2.1 programs of Waters.

RESULTS AND DISCUSSION

MALDI MS Analysis. Matrices common in polymer analysis, such as DIT, DCTB, DHB, and CHCA, were employed both with and without the addition of NaTFA, NaI, or KTFA cationizing salt. In the presence of an alkali metal salt, the major species detected is the free poly(*N*-butylglycine) without the NHC substituent (**4**), which gives rise to a narrow distribution of $[\mathbf{4}_n+Na]^+$ or $[\mathbf{4}_n+K]^+$ ions maximizing near the expected molecular weight (Figure 1). Replacing the trifluoroacetate salt with an iodide salt leads to the same result. In either case, if the detector gain is raised to observe minor products with higher sensitivity, a trace of NHC-poly(*N*-butylglycine), **3**, is also observed in the form of $[\mathbf{3}_n+H]^+$ ions (cf. Figure 1c). Surprisingly, **3**

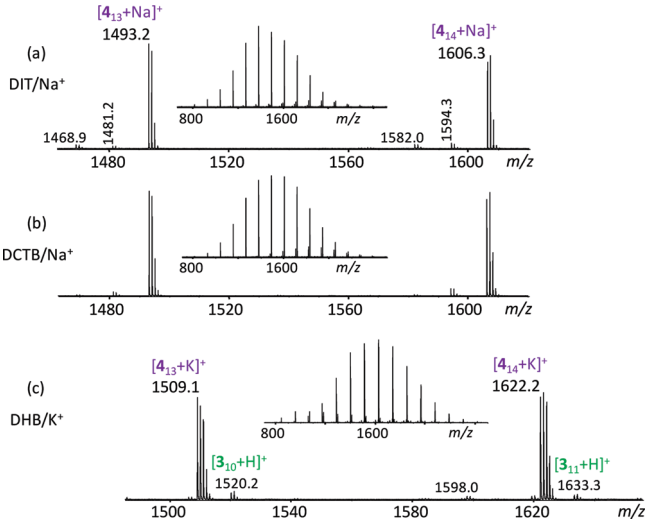

Figure 1. MALDI mass spectra of poly(*N*-butylglycine) 1500, synthesized via NHC-mediated polymerization of *N*-butyl-*N*-carboxyanhydride (Scheme 1) using different matrices and cationizing salts: (a) DIT plus NaTFA; (b) DCTB plus NaTFA; (c) DHB plus KTFA. CHCA gives rise to similar spectra if NaTFA or KTFA is added. An increased detector gain was used for spectrum (c), which distorted the isotope pattern of the main ion series. The m/z values marked in the spectra are for the monoisotopic signals.

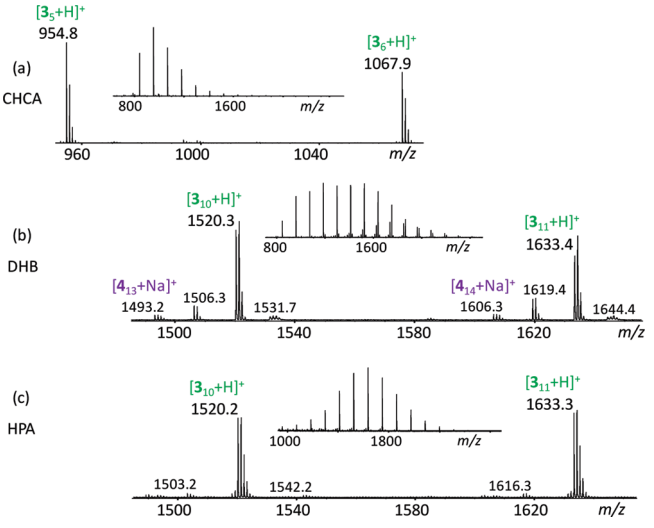

Figure 2. MALDI mass spectra of poly(*N*-butylglycine) 1500, synthesized via NHC-mediated polymerization of *N*-butyl-*N*-carboxyanhydride (Scheme 1) using different matrices but no cationizing salt: (a) CHCA, (b) DHB, and (c) HPA. The molecular weight distribution obtained with HPA most closely agrees with the average molecular weight of ~1500 Da determined by size exclusion chromatography. The m/z values marked in the spectra are for the monoisotopic signals.

becomes the predominant species detected, as a distribution of $[\mathbf{3}_n+\mathrm{H}]^+$ ions, if no salt is added to the sample subjected to MALDI (Figure 2). The highest signal/noise ratio and cleanest spectrum were obtained using HPA as matrix (Figure 2c), presumably because of the low internal energy transferred during protonation with this basic matrix.[44,45] The basicity imparted to **3** by the NHC substituent explains the preference of this product to ionize via proton addition; in contrast, **4** ionizes by metal ion

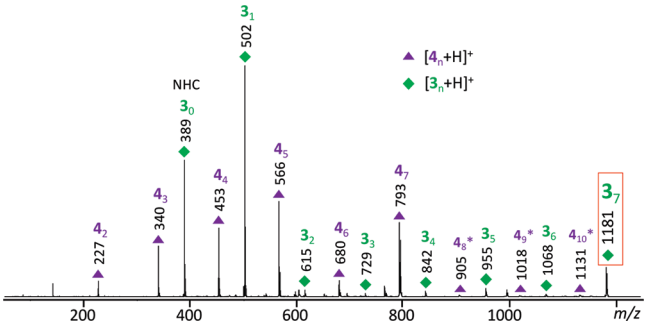

Figure 3. MALDI MS^2 spectrum of the protonated 7-mer from NHC-poly(*N*-butylglycine) 1500 ($[\mathbf{3}_7+\mathrm{H}]^+$ at m/z 1181). The asterisks indicate fragments with more than 7 repeat units.

adduction, as generally do all polyamides.[46] Based on Figure 2, HPA most closely reproduces the average molecular weight of ~1500 determined by NMR or size exclusion chromatography coupled with multiangle light scattering and differential refractive index detection.

The NHC group is a UV chromophore that absorbs at the wavelength of the MALDI laser (355 nm). Therefore, a mass spectrum can be obtained even without a matrix; however, this direct laser desorption causes photoinduced degradation, as the resulting spectrum (not shown) does not contain intact ions of **3** or **4**. Some of the minor, uninterpretable distributions in Figures 1 and 2 could be due to such direct laser desorption/fragmentation.

NHC-mediated ring-opening polymerization is believed to proceed via the zwitterionic intermediate **2**, which is in equilibrium with **3** (Scheme 1). We reason that the anion of the cationizing salt added to the MALDI sample (trifluoroacetate or iodide) catalyzes the conversion **3** → **4** by replacing the NHC chain end of **2** with CF_3COO^- (TFA^-) or I^-, which is subsequently displaced, via intramolecular nucleophilic substitution, by the amide chain end of **2**.[47] A strategy similar to the one used to prepare **3** (Scheme 1) can be applied to lactide to synthesize cyclic polyesters.[34−36] Our MALDI results indicate that the major product in such syntheses is the NHC-substituted macrocycle but that this macrocycle may readily lose the NHC group during MALDI MS analysis, if the analyte sample contains salts, which are often deliberately added to enhance signal intensities. Since NHC-free product is not observed during ESI analysis, even if the sample is doped with an alkali salt (vide infra), the intramolecular nucleophilic substitution must proceed over a considerable barrier that can only be overcome under MALDI, which generally deposits higher average internal energies than the softer ESI method.[44,45]

MALDI MS^2 Characterization of the NHC-Substituted Macrocycle. The protonated 7-mer of NHC-poly(*N*-butylglycine), viz. $[\mathbf{3}_7+\mathrm{H}]^+$ at m/z 1181, was selected for a MALDI MS^2 experiment; the resulting spectrum is shown in Figure 3. When energetically activated, the $[\mathbf{3}_7+\mathrm{H}]^+$ precursor ion dissociates to yield two fragment distributions: one containing NHC-bound poly(*N*-butylglycine) and one free poly(*N*-butylglycine), which have been labeled in Figure 3 by ♦ ($[\mathbf{3}_n+\mathrm{H}]^+$) and ▲ ($[\mathbf{4}_n+\mathrm{H}]^+$), respectively. Dissociation most likely proceeds through the ring-opened isomer (cf. Scheme 2) and involves nucleophilic displacements at the carbonyl groups by the terminal amine to generate $\mathbf{3}_n$ (n = 0−6) and $\mathbf{4}_{7\text{-n}}$ fragments, either of which may keep the proton charge. For instance, bond cleavage at the

dx.doi.org/10.1021/ma200542p |*Macromolecules* 2011, 44, 4555–4564

Scheme 2. Fragmentation of Energetically Activated $[3_7+H]^+$ Ions to Yield Fragments with or without the NHC Moiety[a]

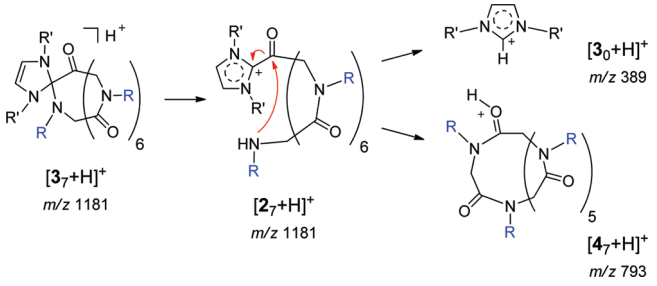

[a] The reaction is exemplified at the C═O group attached to NHC but can similarly occur at the other C═O groups.

carbonyl group next to the NHC substituent would yield the free NHC (3_0) together with 4_7 (Scheme 2), which are observed in protonated form at m/z 389 and 793, respectively. Note that 4_7 is the largest poly(*N*-butylglycine) fragment possible from the heptameric precursor ion selected. Surprisingly, we also observe traces of $[4_n+H]^+$ fragments with more than 7 repeat units (n = 8−10), cf. Figure 3; these are attributed to the presence of isobaric components in the mass-selected $[3_7+H]^+$ precursor ion beam, as will be corroborated by the ESI and TWIM data (vide infra).

ESI MS Analysis. The ESI experiments were performed with a poly(*N*-butylglycine) sample with lower average molecular weight (1100) in order to avoid extensive multiple charging of the polymer, which complicates spectral interpretation. The ions generated by ESI reach the mass analyzing device after passing a desolvation zone and several focusing and guiding lenses; for labile or reactive species, the corresponding temperatures and potentials must be kept low to minimize unintended dissociation (cf. Figure 4). Under such mild conditions, poly(*N*-butylglycine) 1100 gives rise to the spectrum depicted in Figure 4a, in which the main distribution arises from the protonated NHC-carrying polymer, viz. $[3_n+H]^+$. A second distribution, peaking 388 Da higher, corresponds to noncovalent complexes of NHC-poly(*N*-butylglycine) and unreacted NHC, viz. $[3_n+NHC+H]^+$; this distribution disappears at higher temperature and voltage settings (Figure 4b), substantiating that the second NHC unit is attached noncovalently to the protonated oligomers of **3**. The minor distribution observed 22 Da above the major $[3_n+H]^+$ series is due to $[3_n+Na]^+$ ions, originating from adventitious sodium. Supporting evidence for this assignment is provided by the increase in relative intensity of the latter ions when NaTFA is added to the sample (Figure 4c). The added NaTFA also causes some H/Na exchange, which gives rise to $[3_n+2Na-H]^+$ species, cf. Figure 4c; this reaction may proceed by enolization of one amide group, followed by OH → ONa exchange. Addition of NaTFA also reduces the relative abundance of the noncovalent complex. The sodium ion most likely interacts with multiple amide sites of the poly(α-peptoid), leading to a geometry that cannot efficiently associate with a second NHC unit. It is noteworthy that no free poly(*N*-butylglycine) (**4**) is observed in the ESI mass spectra, regardless of whether NaTFA has been added or not. Hence, the presence of NaTFA in the sample is not sufficient to cause the conversion **3** → **4**; higher internal energies are also required. More importantly, the ESI spectra confirm that NHC-mediated

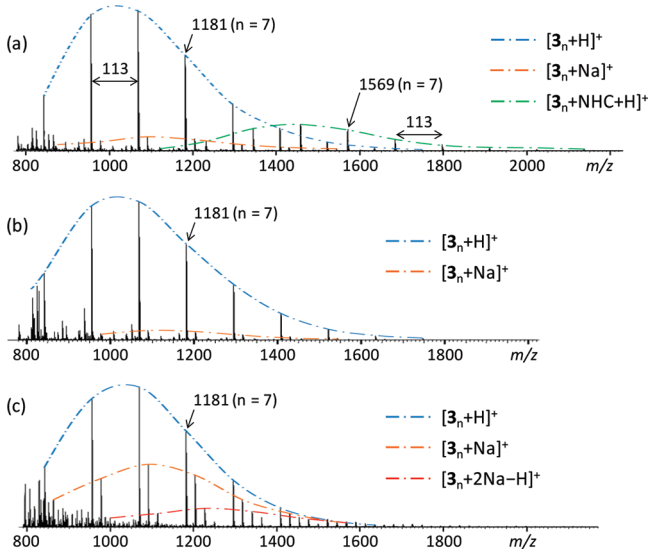

Figure 4. ESI mass spectra of poly(*N*-butylglycine) 1100 acquired (a, b) without or (c) with NaTFA cationizing salt. Other varied parameters: ESI source temperature (a, c) 40 °C or (b) 100 °C; desolvation temperature (a, c) 60 °C or (b) 150 °C; trap cell bias (a, c) 2 V or (b) 6 V; transfer cell bias (a, c) 1 V or (b) 4 V. The m/z values marked in the spectra are for the monoisotopic signals.

ring-opening polymerization produces the NHC-substituted poly(α-peptoid) and that auxiliary reagents (e.g., NaTFA) and energetic excitation (as available in MALDI or MS^2) are necessary to obtain the corresponding free poly(α-peptoid).

ESI MS^2 Characterization of the NHC-Poly(α-peptoid) and Its Noncovalent Adduct with NHC. The ESI MS^2 spectrum of the protonated 7-mer from NHC-poly(*N*-butylglycine), $[3_7+H]^+$ (m/z 1181), shows the same fragment distributions that were observed upon MALDI MS^2 (cf. Figure 5 vs Figure 3). For example, in both cases, cleavage of the NHC group (388 Da) gives rise to major peaks at m/z 793 and 389, corresponding to the complementary fragments $[4_7+H]^+$ (loss of NHC) and $[3_0+H]^+$ (protonated NHC), respectively.

A much simpler MS^2 spectrum is obtained from the complex of the 7-mer and NHC, $[3_7+NHC+H]^+$ (m/z 1569), which mainly dissociates into its constituents, viz. $[3_7+H]^+$ (m/z 1181) and $[NHC+H]^+$ (m/z 389), cf. Figure 6; such fragmentation pattern corroborates that the binding interaction between the NHC-poly(α-peptoid) and the second NHC unit are of noncovalent nature. It is noticed that the ESI MS^2 spectra of both $[3_7+H]^+$ (Figure 5) and $[3_7+NHC+H]^+$ (Figure 6) contain fragments with more than 7 repeat units, some with m/z values above those of the respective precursor ions. This observation indicates that the mass-selected precursor ions (m/z 1181 or 1569) overlap with species in higher charge states (z > 1). More highly charged ions could originate from larger poly(*N*-butylglycine) macrocycles or from products with different, not yet identified structures. The separation ability of TWIM MS, combined with MS^2, will be used to characterize these species.

Separation of the Synthetic Product by ESI-TWIM MS. IM MS and its TWIM MS variant may be viewed as post-ionization chromatography methods that separate gas-phase ions according to their mass, charge, and shape.[19−33] ESI-TWIM MS can be performed on all ions formed upon ESI, or ions of a specific m/z ratio, by setting the quadrupole mass filter preceding the

dx.doi.org/10.1021/ma200542p |*Macromolecules* 2011, 44, 4555–4564

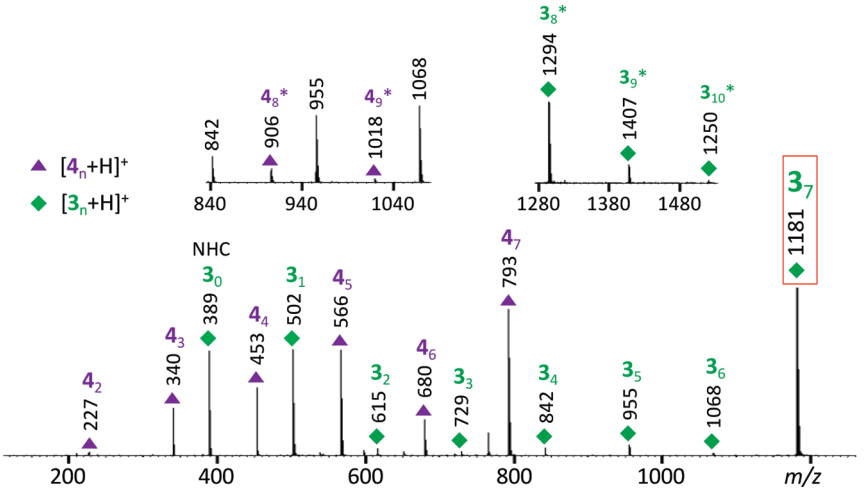

Figure 5. ESI MS^2 spectrum of the protonated 7-mer from NHC-poly(*N*-butylglycine) 1100 ($[\mathbf{3}_7+H]^+$ at *m/z* 1181). The asterisks indicate fragments with more than 7 repeat units.

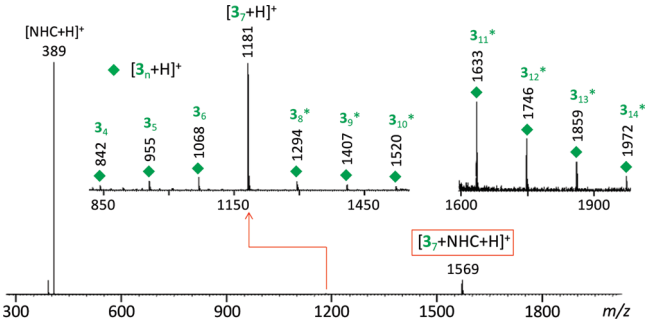

Figure 6. ESI MS^2 spectrum of the protonated cluster containing the 7-mer from NHC-poly(*N*-butylglycine) 1100 and a second NHC unit ($[\mathbf{3}_7+NHC+H]^+$ at *m/z* 1569). The asterisks indicate fragments with more than 7 repeat units.

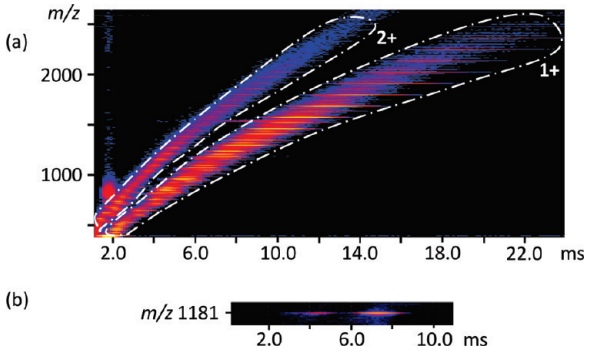

Figure 7. 2-D ESI-TWIM MS plots of (a) all ions and (b) mass-selected *m/z* 1181 from poly(*N*-butylglycine) 1100. The sample was dissolved in methanol (no cationization salt added). The source and desolvation temperatures were set at 40 and 60 °C, respectively.

TWIM region to either rf-only mode or mass-selective mode, respectively.[38,39] Inside the TWIM cell, ions drift under the influence of an electric field against a carrier gas flowing in the opposite direction. Ions of the same mass and charge can be dispersed by shape because the more compact architecture will have a shorter drift time through the TWIM cell. Conversely, different charge states of the same *m/z* ratio can be dispersed by the number of charges because the more highly charged species will travel generally faster in the TWIM cell. The *m/z* values of the separated ions are determined by ToF analysis and (usually) plotted against the corresponding drift times, as shown in Figure 7 for all ions produced by ESI of poly(*N*-butylglycine) 1100 as well as for mass-selected *m/z* 1181.

Two discrete regions of ions are observed in Figure 7a; based on the corresponding isotope patterns, the region with longer drift times (at right) contains singly charged species and the region with shorter drift times (at left) doubly charged species. Each region can be integrated separately to obtain individual mass spectra. The mass spectrum extracted from the 1+ species is similar to that acquired without TWIM (Figure 4a), showing NHC-poly(*N*-butylglycine) ionized by protons, $[\mathbf{3}_n+H]^+$, or sodium ions, $[\mathbf{3}_n+Na]^+$, and the protonated noncovalent complex $[\mathbf{3}_n+NHC+H]^+$. On the other hand, the mass spectrum obtained from the 2+ species (Figure 8) shows five sizable distributions, only two of which are analogous to those detected for +1, viz. $[\mathbf{3}_n+2H]^{2+}$ and $[\mathbf{3}_n+H+Na]^{2+}$. A third distribution arises from the adduct of $\mathbf{3}_n$ and the ESI solvent (methanol), $[\mathbf{3}_n+MeOH+H+Na]^+$, and the remaining two from higher order complexes whose formation unveils important insight into the aggregation/self-assembling properties of NHC-poly(α-peptoid)s (vide infra). Unambiguous detection and identification of the doubly charged products is impossible without prior ion mobility separation due to their small concentration (~5% of total ions).

The TWIM MS plot in Figure 7b illustrates the overlap of different charge states at a given *m/z* ratio. For *m/z* 1181, two distinct components are detected: a major singly charged and a minor doubly charged. The latter constituent reconciles the appearance of tiny fragments with more than 7 repeat units in the MS^2 spectra of $[\mathbf{3}_7+H]^+$ (*m/z* 1181), as was discussed earlier.

The doubly charged distributions of Figure 8 were identified based on their exact *m/z* ratios and, especially, with the help of MS^2 spectra, which will be discussed in detail in the following section. It is important to mention at this point that the yield of 2+ ions depends strongly on the solvent used for ESI. Replacing methanol with an ethanol/acetonitrile mixture essentially eliminates the 2+ charge state (cf. Figure 9). A reduction in the proportion of higher charge states with the use of ACN as solvent had been

dx.doi.org/10.1021/ma200542p |*Macromolecules* 2011, 44, 4555–4564

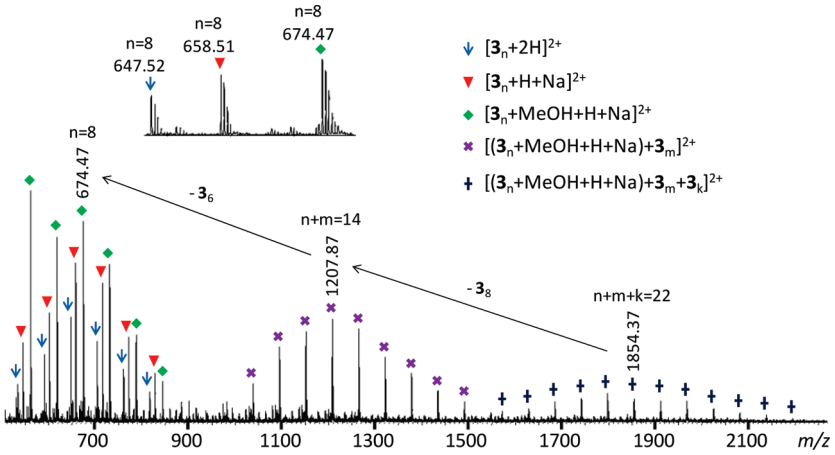

Figure 8. Mass spectrum extracted from the 2+ region in the ESI-TWIM MS plot of poly(*N*-butylglycine) 1100 (Figure 7a). Five doubly charged ion distributions were identified. The inset shows an expanded view of the *m*/*z* 640−680 range. Measured monoisotopic *m*/*z* ratios are given for one species in each distribution; the corresponding calculated *m*/*z* values are 647.49, 658.47, 674.49, 1207.89, and 1854.37, respectively.

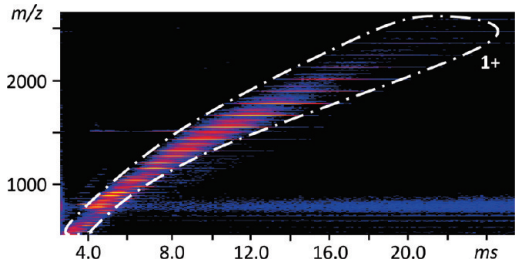

Figure 9. 2-D ESI-TWIM MS plot of poly(*N*-butylglycine) 1100 (all ions), dissolved in EtOH/ACN (v/v, 50/50). No cationization salt was added. The source and desolvation temperatures were set at 40 and 60 °C, respectively.

observed in the ESI mass spectra of proteins and was attributed to the higher basicity of this solvent;[48] such reasoning also reconciles our differences between the ESI data in Figures 7a and 9.

ESI-TWIM MS^2 Characterization of the Higher Order Noncovalent Complexes. The identity of the higher mass distributions with 2+ charges was interrogated by combining TWIM with MS^2. TWIM disperses the singly and doubly charged components of a selected *m*/*z* ratio (precursor ion), so that their MS^2 fragmentation patterns can be examined individually via CAD in the transfer cell that follows the TWIM device. Fragments formed this way have the same drift time as their precursor ions. Those arising from the 2+ component of *m*/*z* 1854, a species in the high mass distribution of Figure 8 (+) are encased in a rectangle in the 2-D TWIM MS^2 plot of Figure 10a; integration of the encased region leads to the ESI-TWIM MS^2 spectrum shown in Figure 10b. All major fragments observed originate from losses of intact NHC-poly(*N*-butylglycine) ($\mathbf{3}_n$) *n*-mers. Repeating the same procedure with doubly charged *m*/*z* 1208, a species in the middle distribution of Figure 8 (×) and a fragment from *m*/*z* 1854, reveals a very similar fragmentation behavior, viz. mainly losses of intact $\mathbf{3}_n$ oligomers (cf. Figure 10c). A dramatically different TWIM MS^2 spectrum is obtained for doubly charged *m*/*z* 674.5 (Figure 10d), a species in the low mass distribution of Figure 8 (◆), and a major fragment from *m*/*z* 1208. There is no loss of intact $\mathbf{3}_n$ oligomers; instead, NHC elimination gives rise to the most abundant signal, and most other fragmentation pathways lead to singly or doubly charged $\mathbf{4}_n$ (NHC-free poly(*N*-butylglycine)). These MS^2 characteristics provide convincing evidence that the 2+ products of intermediate (×) or high (+) mass in Figure 8 correspond to noncovalent complexes, assembled from a core unit plus either one or two $\mathbf{3}_n$ units, respectively. The core is composed of $\mathbf{3}_n$ + MeOH and is doubly charged by H^+ and Na^+ (labeled by ◆ in Figure 8). The 2+ distribution without MeOH or that ionized by two protons (↓ and ▼, respectively, in Figure 8) form no association products. Evidently, both MeOH and sodium are required to promote self-assembly. The exact structure of the core remains puzzling.

Is the Poly(α-peptoid) Formed after NHC Release Cyclic? Our study with NHC-containing poly(*N*-butylglycine) has shown that such poly(α-peptoid)s can readily lose the NHC substituent either unintentionally, due to the sample preparation procedure used, or intentionally, by activation with collisions or laser light during MS^2 experiments. On the basis of their mass, the resulting NHC-free poly(α-peptoid)s carry no end groups and, thus, have been assumed to be macrocyclic; however, isomeric linear structures with one saturated and one unsaturated chain end are also possible. For an unequivocal determination of the correct architecture, the poly(*N*-methylglycine) generated from the corresponding NHC-containing polymer was compared to an isomer, viz. cyclic poly(alanine), which was prepared by a method known to yield the cyclic polypeptide. ESI-TWIM MS of the poly(alanine) sample led to the 2-D plot depicted in Figure 11a, in which protonated oligomers, $[(Ala)_n+H]^+$, are the dominant ions (Ala abbreviates the repeat unit of alanine). NHC-free poly(*N*-methylglycine), produced by MS^2 (CAD) of the corresponding NHC-containing product in the cell preceding the TWIM device (see Experimental Section), led to the 2-D plot depicted in Figure 11b, where protonated oligomers also dominate. The drift times of isomers with the same number of repeat units are identical within experimental error. Also, the corresponding drift time distributions are indistinguishable, as attested for the 6-, 7-, and 8-mers in the respective figure insets. These results clearly indicate that poly(alanine) and poly(*N*-methylglycine) *n*-mers of the same size have essentially the same geometries (collision cross sections).[19−26,29−31,33]

Linear poly(*N*-methylglycine) isomers would have had considerably longer drift times because of their extended geometries

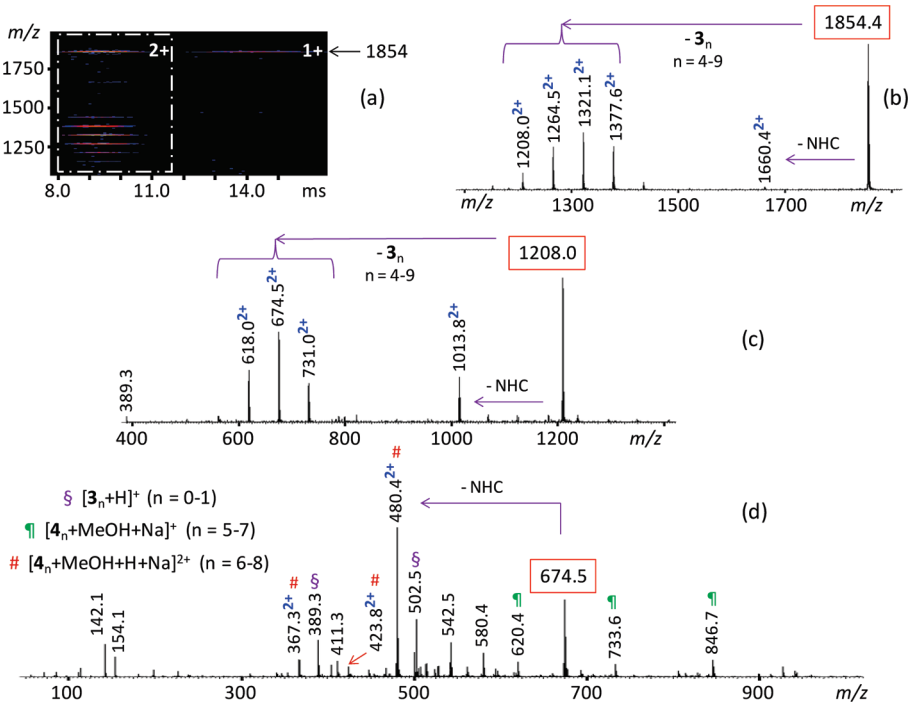

Figure 10. (a) 2-D ESI-TWIM MS^2 plot of the m/z 1854 ion from poly(*N*-butylglycine) 1100 dissolved in MeOH and (b) ESI-TWIM MS^2 mass spectrum of doubly charged m/z 1854 extracted from the encased region of the plot. (c, d) ESI-TWIM MS^2 mass spectra of doubly charged (c) m/z 1208 and (d) 674.5 extracted from analogous 2-D TWIM MS^2 plots (not shown). Doubly charged fragments are indicated by a 2+ superscript. The ions at m/z 142.1, 154.1, 542.5, and 580.4 in part (d) agree well with $(butyl)_2N^+{=}CH_2$, [*N*-butylglycine+Na]$^+$, [$\mathbf{3}_1$+H_2O+Na]$^+$, and [$\mathbf{4}_5$+Me]$^+$, respectively.

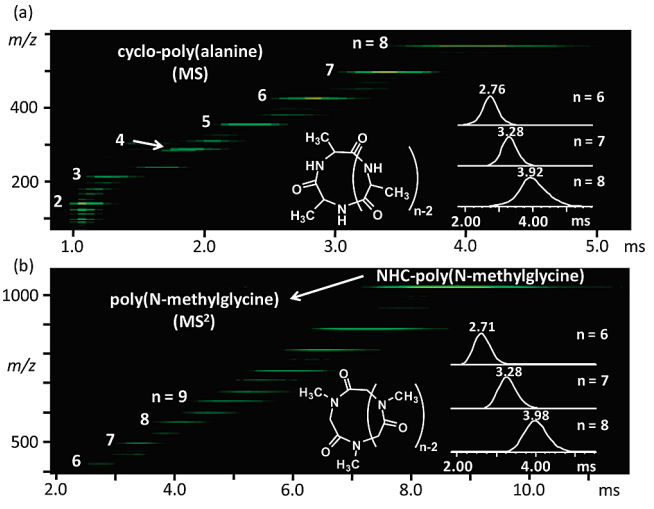

Figure 11. (a) 2-D ESI-TWIM MS plot of poly(alanine) (all ions formed upon ESI) and (b) 2-D ESI MS^2-TWIM plot of the protonated 9-mer from NHC-poly(*N*-methylglycine) (m/z 1028.6). Both plots were acquired at the same TWIM conditions (traveling wave velocity of 350 m/s and traveling wave height of 8.5 V). The samples were dissolved in methanol (acidified by trifluoroacetic acid); source and desolvation temperatures were set at 40 and 60 °C, respectively.

(larger collision cross sections).[49,50] Our TWIM MS/MS^2 findings confirm that NHC release leads to macrocyclic poly(α-peptoid)s in the gas phase of the mass spectrometer. This dissociation likely proceeds via acid-catalyzed, intramolecular nucleophilic substitution, as rationalized in Scheme 2. Solvents that favor such an intramolecular (and, hence, unimolecular) pathway should also yield macrocyclic poly(α-peptoid) architectures in solution.

SUMMARY

Mass spectrometry advancements in the past two decades have substantially facilitated the characterization of synthetic polymers. This Perspective illustrated how multiple levels of mass spectrometry can be applied to gain comprehensive insight into the composition, structure, and architecture of a promising class of biomimetic materials, viz. poly(α-peptoid)s.

Without mass spectrometry analysis, it is difficult to conclusively deduce the real compositional heterogeneity of polymers. MALDI still is the most straightforward and widely used tool to obtain this information because it produces mainly singly charged ions minimizing superimposed charge states, has a high tolerance for impurities and salts, and provides analysis with high sensitivity and speed. Inappropriate matrix and salt selection can, however, introduce erroneous results, especially for labile species. Our experiments with poly(*N*-butylglycine) clearly show that the acquisition of spectra under a variety of experimental conditions are advisible to ensure that the polymer is not changed during the MALDI MS analysis. Compared to MALDI, ESI is softer and more suitable for labile materials, especially for products held together by noncovalent interactions. It also introduces multiple charging which may complicate the resulting spectra, but which also allows for the detection of products of high molecular weight that might escape detection in charge state 1+ (or 1−) due to mass discrimination effects. MS analysis can be further enhanced by ion mobility spectrometry and tandem mass spectrometry. The former enables separation by charge state and/or architecture, making it possible to identify minor or overlapping components invisible in the total spectrum, while the latter confirms primary structure and the presence or absence of noncovalent interactions (which are weak and, hence, break most

dx.doi.org/10.1021/ma200542p |*Macromolecules* 2011, 44, 4555–4564

easily). Combining ion mobility separation with tandem MS further allows for the simultaneous separation and determination of polymer architectures. Here, all these top-down approaches have been employed to prove beyond doubt that NHC-mediated zwitterionic ring-opening polymerization yields products carrying the NHC functionality and that elimination of this NHC substituent opens a route to cyclic poly(α-peptoid)s having conformations that closely mimic those of cyclic polypeptides. At the same time, this study warns that, although mass spectrometry plays a vital role in synthetic polymer analysis, it may alter the analyte, yielding misleading data; the use of more than one approach is recommended to avoid such pitfalls.

AUTHOR INFORMATION

Corresponding Author
*E-mail: wesdemiotis@uakron.edu.

BIOGRAPHIES

Xiaopeng Li received his B.S. degree in chemistry from Zhengzhou University, China, in 2004. After completing his Ph.D. in Clinical/Bioanalytical Chemistry with Dr. Baochuan Guo at Cleveland State University in 2008, he joined the Mass Spectrometry Center at the University of Akron under the direction of Dr. Chrys Wesdemiotis. His current research focuses on investigations of polymers, supramolecules, and supramolecular polymers using MALDI, ESI, and ion mobility mass spectrometry.

Li Guo received her B.S. degree in Chemistry from Zhengzhou University, China. She obtained her Ph.D. degree in Polymer Chemistry and Physics in 2007 with Prof. Zhijie Zhang at the Institute of Chemistry, Chinese Academy of Sciences, China. She is currently a postdoctoral research associate with Prof. Donghui Zhang in the Department of Chemistry at Louisiana State University. Her postdoctoral research focuses on the synthesis and characterization of polypeptides and polypeptoids.

Madalis Casiano-Maldonado studied chemistry at the Pontifical Catholic University of Puerto Rico, where she received a B.S. degree in 2005. Currently, she is a Ph.D. candidate in the Department of Chemistry at The University of Akron. Her dissertation research involves the characterization of enzyme-digested high molecular weight polymers and the quantitative analysis of protein adsorption on polymer surfaces using MALDI and ESI mass spectrometry techniques. In 2010, she was the recipient of Henry Stevens scholarship granted by Akron Chemistry Department.

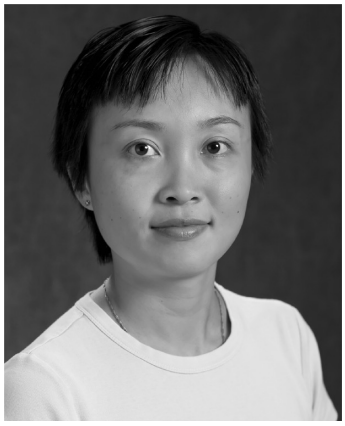

Donghui Zhang is an assistant professor in the Department of Chemistry and the Macromolecular Studies Group at the Louisiana State University in Baton Rouge, LA. She was born and raised in Beijing, P. R. China. After obtaining a B.S. degree in chemistry from Peking University in 1998, she moved to the U.S. and enrolled in the chemistry graduate program at Dartmouth College, where she completed her Ph.D. degree in 2003. She did postdoctoral research at the University of Minnesota on the synthesis and characterization of polymers from biorenewable feedstock. She joined LSU in 2007 after a two-year stint as a research professor at New Mexico State University where her research was focused on carbon nanotube composites. Her current research interests include polymerization catalysis toward peptidomimetic polymers and the design and synthesis of polypeptide and polypeptoid-based functional materials.

Chrys Wesdemiotis received his Ph.D. degree with Helmut Schwarz at Technische Universität Berlin in 1979. He was a postdoctoral fellow with Fred W. McLafferty at Cornell University in 1980. After completing his military service in Greece (1981−1983), he returned to Cornell as a senior research associate (1983−1989). In 1989, he joined the faculty of the University of Akron, where he currently is Distinguished Professor of Chemistry, Polymers Science, and Integrated Bioscience. Research in the Wesdemiotis group focuses on the development and applications of multidimensional mass spectrometry methods for the characterization of new synthetic polymers and polymer−biomolecule interfaces.

■ ACKNOWLEDGMENT

We acknowledge generous financial support from the National Science Foundation (Grants CHE-0517909, CHE-1012636, and DMR-0821313 to C.W. and grant CHE-0955820 to D.Z.) and from the Louisiana State Board of Regents (Grant LEQSF-RD-A-11 to D.Z.).

■ REFERENCES

(1) Karas, M.; Hillenkamp, F. *Anal. Chem.* **1988**, *60*, 2299–2301.
(2) Tanaka, K.; Waki, H.; Ido, S.; Akita, Y.; Yoshida, Y.; Yoshida, T. *Rapid Commun. Mass Spectrom.* **1988**, *2*, 151–153.
(3) Fenn, J. B.; Mann, M.; Meng, C. K.; Wong, S. F.; Whitehouse, C. M. *Science* **1989**, *246*, 64–71.
(4) Hanton, S. D. *Chem. Rev.* **2001**, *101*, 527–569.
(5) Montaudo, G., Lattimer, R. P., Eds.; *Mass Spectrometry of Polymers*; CRC Press: Boca Raton, FL, 2002.
(6) McEwen, C. N.; Peacock, P. M. *Anal. Chem.* **2002**, *74*, 2743–2748.
(7) Murgasova, R.; Hercules, D. M. *Anal. Bioanal. Chem.* **2002**, *373*, 481–489.
(8) Pasch, H.; Schrepp, W. *MALDI-TOF Mass Spectrometry of Synthetic Polymers*; Springer: Berlin, 2003.
(9) Peacock, P. M.; McEwen, C. N. *Anal. Chem.* **2004**, *76*, 3417–3428.
(10) Arnould, M. A.; Polce, M. J.; Quirk, R. P.; Wesdemiotis, C. *Int. J. Mass Spectrom.* **2004**, *238*, 245–255.
(11) Peacock, P. M.; McEwen, C. N. *Anal. Chem.* **2006**, *78*, 3957–3964.
(12) Weidner, S. M.; Trimpin, S. *Anal. Chem.* **2008**, *80*, 4349–4361.
(13) Weidner, S. M.; Trimpin, S. *Anal. Chem.* **2010**, *82*, 4811–4829.
(14) Gruendling, T.; Weidner, S.; Falkenhagen, J.; Barner-Kowollik, C. *Polym. Chem.* **2010**, *1*, 599–617.
(15) Jackson, A. T.; Bunn, A.; Chisholm, S. *Polymer* **2008**, *392*, 575–583.
(16) Crecelius, A. C.; Baumgaertel, A.; Schubert, U. S. *J. Mass Spectrom.* **2009**, *44*, 1277–1286.
(17) Polce, M. J.; Wesdemiotis, C. In *MALDI Mass Spectrometry for Synthetic Polymer Analysis*; Li, L., Ed.; John Wiley & Sons: Hoboken, NJ, 2010; Chapter 5, pp 85−127.
(18) Wesdemiotis, C.; Solak, N.; Polce, M. J.; Dabney, D. E.; Chaicharoen, K.; Katzenmeyer, B. C. *Mass Spectrom. Rev.* **2011**10.1002/mas.20282.
(19) Von Helden, G.; Hsu, M.-T.; Kemper, P. R.; Bowers, M. T. *J. Chem. Phys.* **1991**, *95*, 3835–3837.
(20) Bowers, M. T.; Kemper, P. R.; von Helden, G.; Koppen, P. A. M. *Science* **1993**, *260*, 1446–1451.
(21) Clemmer, D. E.; Jarrold, M. F. *J. Mass Spectrom.* **1997**, *32*, 577–592.
(22) Verbeck, G. F.; Ruotolo, B. T.; Sawyer, A. A.; Gillig, K. J.; Russell, D. H. *J. Biomol. Tech.* **2002**, *13*, 56–61.
(23) Trimpin, S.; Plasencia, M.; Isailovic, D.; Clemmer, D. E. *Anal. Chem.* **2007**, *79*, 7965–7974.
(24) Bohrer, B. C.; Merenbloom, S. I.; Koeniger, S. L.; Hilderbrand, A. E.; Clemmer, D. E. *Annu. Rev. Anal. Chem.* **2008**, *1*, 293–327.
(25) Trimpin, S.; Clemmer, D. E. *Anal. Chem.* **2008**, *80*, 9073–9083.
(26) Anderson, S. E.; Bodzin, D. J.; Haddad, T. S.; Boatz, J. A.; Mabry, J. M.; Mitchell, C.; Bowers, M. T. *Chem. Mater.* **2008**, *20*, 4299–4309.
(27) Hilton, G. R.; Jackson, A. T.; Thalassinos, K.; Scrivens, J. H. *Anal. Chem.* **2008**, *80*, 9720–9725.
(28) Gies, A. P.; Kliman, M.; McLean, J. A.; Hercules, D. M. *Macromolecules* **2008**, *41*, 8299–9301.
(29) Chan, Y.-T.; Li, X.; Soler, M.; Wang, J. L.; Wesdemiotis, C.; Newkome, G. R. *J. Am. Chem. Soc.* **2009**, *131*, 16395–16397.
(30) Perera, S.; Li, X.; Soler, M.; Schultz, A.; Wesdemiotis, C.; Moorefield, C. N.; Newkome, G. R. *Angew. Chem., Int. Ed.* **2010**, *49*, 6539–6544.
(31) Brocker, E. R.; Anderson, S. E.; Northrop, B. H.; Stang, P. J.; Bowers, M. T. *J. Am. Chem. Soc.* **2010**, *132*, 13486–13494.
(32) Ren, X.; Sun, B.; Tsai, C.-C.; Tu, Y.; Leng, S.; Li, K.; Kang, Z.; Van Horn, R. M.; Li, X.; Zhu, M.; Wesdemiotis, C.; Zhang, W.-B.; Cheng, S. Z. D. *J. Phys. Chem. B* **2010**, *114*, 4802–4810.
(33) Li, X.; Chan, Y.-T.; Newkome, G. R.; Wesdemiotis, C. *Anal. Chem.* **2011**, *83*, 1284–1290.
(34) Culkin, D. A.; Jeong, W.; Csihony, S.; Gomez, E. D.; Balsara, N. P.; Hedrick, J. L.; Waymouth, R. M. *Angew. Chem., Int. Ed.* **2007**, *46*, 2627–2630.
(35) Jeong, W.; Hedrick, J. L.; Waymouth, R. M. *J. Am. Chem. Soc.* **2007**, *129*, 8414–8415.
(36) Jeong, W.; Shin, E. J.; Culkin, D. A.; Hedrick, J. L.; Waymouth, R. M. *J. Am. Chem. Soc.* **2009**, *131*, 4884–4891.
(37) Guo, L.; Zhang, D. *J. Am. Chem. Soc.* **2009**, *131*, 18072–18074.
(38) Giles, K.; Pringle, S. D.; Worthington, K. R.; Little, D.; Wildgoose, J. L.; Bateman, R. H. *Rapid Commun. Mass Spectrom.* **2004**, *18*, 2401–2414.
(39) Pringle, S. D.; Giles, K.; Wildgoose, J. L.; Williams, J. P.; Slade, S. E.; Thalassinos, K.; Bateman, R. H.; Bowers, M. T.; Scrivens, J. H. *Int. J. Mass Spectrom.* **2007**, *261*, 1–12.
(40) Shvartsburg, A. A.; Smith, R. D. *Anal. Chem.* **2008**, *80*, 9689–9699.
(41) Hilton, G. R.; Thalassinos, K.; Grabenauer, M.; Sanghera, N.; Slade, S. E.; Wyttenbach, T.; Robinson, P. J.; Pinheiro, T. J. T.; Bowers, M. T.; Scrivens, J. H. *J. Am. Soc. Mass Spectrom.* **2010**, *21*, 845–854.
(42) Zhou, N.; Lu, K.; Liu, Y.; Chen, Y.; Tang, G.; Cao, S.-X.; Qu, L.-B.; Zhao, Y.-F. *Rapid Commun. Mass Spectrom.* **2002**, *16*, 919–922.
(43) Suckau, D.; Resemann, A.; Schuerenberg, M.; Hufnagel, P.; Franzen, J.; Holle, A. *Anal. Bioanal. Chem.* **2003**, *376*, 952–965.
(44) Knochenmuss, R. In *Electrospray and MALDI Mass Spectrometry: Fundamentals, Instrumentation, Practicalities, and Biological Applications*, 2nd ed.; Cole, R. B., Ed.; John Wiley & Sons: Hoboken, NJ, 2010; Chapter 5, pp 149−183.
(45) Hossain, M.; Limbach, P. A. In *Electrospray and MALDI Mass Spectrometry: Fundamentals, Instrumentation, Practicalities, and Biological Applications*, 2nd ed.; Cole, R. B., Ed.; John Wiley & Sons: Hoboken, NJ, 2010; Chapter 7, pp 215−244.

(46) Puglisi, C.; Samperi, F.; Di Giorgi, S.; Montaudo, G. *Macromolecules* **2003**, *36*, 1098–1107.
(47) Smith, M. B.; March, J. *March's Advanced Organic Chemistry: Reactions, Mechanisms, and Structure*, 5th ed.; John Wiley & Sons: New York, 2001; p 427.
(48) Iavarone, A. T.; Jurchen, J. C.; Williams, E. R. *J. Am. Soc. Mass Spectrom.* **2001**, *11*, 976–985.
(49) Ruotolo, B. T.; Tate, C. C.; Russell, D. H. *J. Am. Soc. Mass Spectrom.* **2004**, *15*, 870–878.
(50) Riba-Garcia, I.; Giles, K.; Bateman, R. H.; Gaskell, S. J. *J. Am. Soc. Mass Spectrom.* **2008**, *19*, 609–613.